Optics Communications 287 (2013) 145–149

Contents lists available at SciVerse ScienceDirect

Optics Communications

journal homepage: www.elsevier.com/locate/optcom

Optical properties of non-linear crystal grown from the melt GaSe–$AgGaSe_2$

J.-J. Xie [a], J. Guo [a], L.-M. Zhang [a], D.-J. Li [a], G.-L. Yang [a], F. Chen [a], K. Jiang [a], M.E. Evdokimov [b], M.M. Nazarov [b], Yu.M. Andreev [c,e], G.V. Lanskii [c,e], K.A. Kokh [d,*], A.E. Kokh [d], V.A. Svetlichnyi [e]

[a] State Key Laboratory of Laser Interaction with Matter, Changchun Institute of Optics, Fine Mechanics and Physics of CAS, 3888, Dongnanhu Road, Changchun 130033, China
[b] Physics Department, Moscow State University, 1/Bld. 62, Leninskie Gory, Moscow 119991, Russia
[c] Laboratory of Geosphere–Biosphere Interactions, Institute of Monitoring of Climatic and Ecological Systems of SB RAS, 10/3, Academichesky Avenue, Tomsk 634055, Russia
[d] Laboratory of Crystal Growth, Institute of Geology and Mineralogy of SB RAS, 3, Koptyuga Avenue, Novosibirsk 630090, Russia
[e] Laboratory of Advanced Materials and Technologies, Siberian Physical-Technical Institute of Tomsk State University, 1, Novosobornaya Square, Tomsk 634050, Russia

ARTICLE INFO

Article history:
Received 26 May 2012
Received in revised form
22 August 2012
Accepted 14 September 2012
Available online 29 September 2012

Keywords:
GaSe
Doping
Crystal growth
Optical propeties

ABSTRACT

Modified GaSe single crystal was grown from the melt with charge composition GaSe+10 mass% of $AgGaSe_2$. Lattice structure, visible to mid-IR and further THz range optical properties, as well as Raman spectra were studied in details. The grown crystal was identified as ε-GaSe:Ag (0.04 mass%). This silver content in GaSe has resulted in 6% decreased non-linearity that was over compensated in CO_2 laser SHG efficiency by vanished of bulk damages and 10–20% improved surface damage threshold. About 30% increased microhardness is promising for cut and polishing at arbitrary direction and ε-GaSe:Ag applications in out-of-door systems.

1. Introduction

Layered GaSe was proposed as a new prospective non-linear material in 1972 [1]. Till recently, in parallel with [2–5] and in spite of something lower figure of merit to that in $ZnGeP_2$ [2], GaSe has demonstrated impressive results in frequency conversion within mid-IR [2,6,7]. Special attention was paid to design of all-solid-state state laser systems and frequency converters of high efficiency and output power CO_2 lasers. First analysis of CO_2 laser frequency conversion (namely SHG) in GaSe was reported in [8]. Comparative analysis of GaSe and of other non-linear material efficiencies as CO_2 laser SHG is presented in [9]. Summarized data on frequency conversion, relation of achieved results with physical properties and perspectives for future research of GaSe are considered in the circumstantial paper of Allakhverdiev et al. [10].

During last decade GaSe also ranked among most efficient materials for frequency converters into THz and further into millimeter ranges [11–15]. New types of frequency converters, in particular up-converter of THz emission into near IR [16], and all-solid-state portable THz source [17] were also designed. Comparative analysis of GaSe and other crystal efficiencies in frequency conversion into THz range is carried out in [18,19]. Frequency conversion of CO_2 laser into long wavelength range was again of special interest due to well known Manly–Rowe relation [20] that predicts linear increase in frequency conversion efficiency with enlarge of pump beam wavelength.

Thus, in the literature, layered ε-GaSe appears to be one of the most promising materials for mid-IR and THz generation and tuning. On the other hand, real efficiency of frequency conversion and applications are limited by state-of-the art of GaSe growth technology (absorption coefficient at mid-IR maximal transparency range is often between 0.25 cm^{-1} and 0.1 cm^{-1} [21]) and low mechanical properties originated from the layered structure. Grown ε-GaSe crystals possess numerous point (Ga vacancies dominates), micro-(precipitations) and stacking defects, often contain admixture of other (γ, δ and β) polytypes and demonstrate decrease in efficient non-linearity with an increase of the crystal length (so called scaling-up effect) [22]. Besides, these disadvantages lead to highly variable data on its physical properties in the literature.

Fortunately, GaSe lattice well incorporates different doping elements with significant modification of mechanical and other physical properties that are responsible for efficiency of frequency conversion. For the first time over 35% improvement of the efficient non-linearity in GaSe (80% in CO_2 laser SHG efficiency in the 4 mm crystal) was obtained by doping with In atoms [22] that was confirmed later in [23]. It was ascertained that the increase of non-linearity coefficient towards intristic value of $d_{22}=70$ pm/V was due to the improvement of optical quality of

* Corresponding author. Tel./fax: +7 383 3066392.
E-mail address: k.a.kokh@gmail.com (K.A. Kokh).

0030-4018/$ - see front matter © 2012 Elsevier B.V. All rights reserved.
http://dx.doi.org/10.1016/j.optcom.2012.09.034

the crystal. Then Hsu et al. [24] have reported 24% increase of intrinsic non-linearity caused by 0.5 at% doping of Er atoms. In the early 80's Allakhverdiev et al. [25] have shown that addition of lighter atoms of S in the GaSe results in the decrease of d_{22} coefficient. However, it was latter established that the set of modified physical properties of S-doped GaSe results in the 2.4-fold increase in YAG:Er^{3+} laser SHG efficiency [26]. Simultaneously, mechanical properties were improved significantly which have allowed easier cut and polishing [23,25,27] and exploitation in out-of-door devices [28]. Besides, damage threshold increased in parallel appears an easy way to increase conversion efficiency.

On a par with the doping by single-type atoms it is evident that introduction of several impurities in the crystallizing melt would also result in some change of crystal properties. Recently, the GaSe:S,Ag crystal was grown from the complex composition melt of GaSe:$AgGaS_2$ (10.6 mass%) [29]. The single crystalline part of the ingot had almost identical efficiency in CO_2 laser SHG to that of GaSe:S (2 mass%) grown with conventional doping by sulfur under same pump intensity [30–33] but improved hardness [34]. Singh et al. [35] had established that the crystal grown from GaSe:$AgGaSe_2$ (10.4 mass%) melt possesses highest non-linearity coefficient of 75 pm/V among known doped GaSe crystals. However, there is still no further information about the real composition, structure, optical properties and phase matching for the crystal grown in the system GaSe–$AgGaSe_2$. The goal of this work was to study in details chemical composition, crystal structure, optical properties and damage threshold of the crystal grown from the melt GaSe:$AgGaSe_2$ (10 mass%).

2. Experimental

GaSe charge was synthesized from high purity (5 N) elementary Ga and Se. About 150 g of polycrystalline material was prepared by the modified synthesis procedure well described in [36]. For doping a charge of 10 mass% of stoichiometric $AgGaSe_2$ compound was added to presynthesized GaSe similar to that reported in Ref. [37]. The whole charge was loaded to the growth ampoule which was sealed off after evacuation down to 10^{-4} Torr. Single crystal growth was performed by modified Bridgman method under heat field rotation conditions [38]. The vertical temperature gradient at the crystallization front was 10 deg/cm and crystal pulling rate was 10 mm/day. Both doped and pure GaSe crystals were grown by this technique. All z-cut samples studied were cleaved from the nose and middle parts of the as-grown ingots and were used without any additional treatment.

Composition of the doped crystal was measured by electron probe microanalysis (EPMA) with averaging over an area $100 \times 100\ \mu m^2$ that reveals clear signal of selenium and gallium, but no signal related to silver in GaSe:$AgGaSe_2$. Silver content was probed by atomic-absorption spectrometry with Z-8000, Hitachi spectrometer (air–acetylene flame). Structural property of the crystal was observed by transmission electron microscopy (TEM) with TESLA BS-513A microscope at electron accelerating voltage 100 kV. Raman scattering spectra were recorded by IR Raman Fourier spectrometer Nicolet NXR 9650 (Thermo Electron Corp., USA): $\Delta\lambda = 3500–100\ cm^{-1}$, spectral resolution 0.8 cm^{-1} under Nd:YAG laser pump at 1.064 μm. The hardness of the samples was measured with CSEM Nano Hardness Tester.

UV–visible absorption spectra of the samples were recorded by Cary 100 Scan (Varian, Inc., Austria) spectrometer: wavelength range 190–900 nm, spectral resolution $\Delta\lambda = 0.2–4$ nm, wavelength deviation ± 1 nm. Mid-IR optical depths were recorded by FTIR Nicolet 6700 (Thermo Electron Corp.) spectrometer: operation wavelength range 11,000–375 cm^{-1}, spectral resolution 0.09 cm^{-1}. Terahertz range o-wave dispersions n_o and absorption spectra were recorded by home-made THz-TDS spectrometer with 50 fs Ti:Sapphire laser system (797 nm) described else where [39]. THz beam was normally incident to the crystal face. To check the consistence of this study data, first experimental results obtained for pure GaSe were compared with the calculated results obtained with dispersion equations recommended in Ref. [2]. Compared results were good well in coincidence. Then the measurement was carried out for GaSe:$AgGaSe_2$ crystals.

The second harmonic generation efficiency in z-cut GaSe and GaSe:$AgGaSe_2$ samples were determined using low pressure tunable CO_2 laser: pulse repletion frequency 400–600 Hz, pulse duration 250 ns and peak power of 1–3 kW as a pump source. By cleaving the as-grown ingots the samples with interaction lengths of 2 ± 0.02 mm and 5.3 ± 0.04 mm were prepared from available GaSe of different optical quality and grown GaSe:$AgGaSe_2$ crystals. Also 2 mm and 5.3 mm long $ZnGeP_2$ samples without antireflection coating were applied in the experimental study for comparison. $ZnGeP_2$ crystals were cut and polished for I-type CO_2 laser SHG ($\theta = 77°$, $\varphi = 0°$) and characterized by $\alpha \approx 0.1\ cm^{-1}$ at the maximal transparency range 2.5–8.3 μm and $\alpha \approx 0.7\ cm^{-1}$ at 9.3 μm CO_2 laser line. SHG pulses were recorded by highly sensitive RT pyroelectric detector MG-30, Russia, NPO Vostok ($D = 7 \times 10^8\ cm\ Hz^{1/2}/W$ at 2–20 μm range) with built-in selective preamplifier. Output signals were measured by selective nanovoltmeter Unipan-237, Poland (10 Hz spectral bandwidth) and displayed with TDS 3052 (Tektronics) oscilloscope for visual control.

3. Results and discussion

The optical quality of the doped crystal appeared to be very good when viewed with the unaided eye, and the entire optical aperture was found to be very uniform in the optical quality part of the boule (Fig. 1). Any Ag-rich precipitations in the samples were not observed, so as in [35] for Ag concentration lower than 5000 ppm. Also, no intensive segregation of Ag into the tail part of the ingot was observed in difference to GaSe:$AgGaS_2$ ingot which is described in [29,34]. The composition of the grown crystal was identified as GaSe:Ag with the following contents: Ga 44.59 mass%, Se 55.37 mass% and Ag 0.04 mass%. We were able to define only upper limit of Ag-content due to low level signal depending on the sample location in the ingot. Nevertheless, this

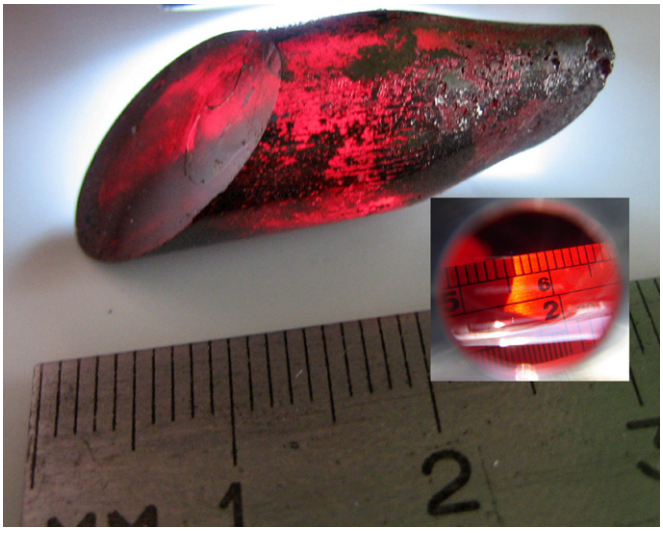

Fig. 1. External view on the grown crystal from the melt GaSe–$AgGaSe_2$ (10 mass%). A view through 5 mm sample is shown in the figure inset.

small content of silver results in the increased hardness of GaSe:Ag crystal (≥ 10.7 kg/mm^2) which is $\sim$30% higher to that of 8 kg/mm^2 for pure GaSe. This phenomenon is possibly due to Ga vacancy occupation and/or intercalation between primitive layers by the Ag atoms.

Only ε-GaSe crystalline phase was detected by TEM observation both in pure and Ag-doped GaSe crystals. The electron diffraction patterns confirm high quality of pure GaSe lattice: reflexes are round and symmetrically disposed circles. The electron diffraction patterns for the optical quality part of the GaSe:Ag ingot was evidently also attributed to the ε-GaSe structure. Diffraction patterns of GaSe:Ag were a bit deformed (polar splitting angle is $<0.3^\circ$) due to the presence of Ag impurity or small admixture of other polytypes whose reflexes significantly overlapped with ε-GaSe reflexes. The splitting angle was smoothly increasing upto $\sim 1^\circ$ to the tail part of the ingot which is likely to be a result of slight segregation of Ag along the crystal. The ε-polytype structure of the GaSe:Ag samples was also confirmed by non-linear optical method by observing φ-angle dependence of CO_2 laser I-type SHG signal [40]. For all samples the SHG signal for the I-type interaction versus φ-angle in polar coordinates was the clear six-petal-flower type and no phase matching was found at 90° and 270°, which is in agreement with the relation for efficient nonlinear susceptibility coefficient $d_{eff}=d_{22}\cos\theta \sin 3\varphi$ in ε-GaSe. It has to be noted that this method did not allow identifying presence of β-polytype GaSe. Besides, the identity of crystal structures of GaSe and GaSe:Ag may be illustrated by close identity of Raman spectra structure for GaSe and GaSe:Ag presented in Fig. 2. Another point should be considered in the spectra is a transformation in the shape form of the E′-doublet peak at 212 cm^{-1}. The ε-polytype structure has a D_{3h} point-group symmetry with two layers (four molecules) per unit cell. This doublet peak originates from Ga–Se vibrations and reflects layer-to-layer interaction within unit cell (Davydov splitting) [41,42]. The splitting yields doublet. In Fig. 2 it is just noticeable for GaSe and well observable for GaSe:Ag. It can be proposed that these changes are caused by stronger bounding between primitive layers in GaSe mainly due to interlayer intercalation by silver atoms.

UV and mid-IR absorptivity spectra of the samples are shown in Fig. 3. Calibration of these spectra was performed by making the measurement at chosen points on the crystal face with low power ∅1.0 mm beam at 9.3 μm emission line of CO_2 laser to minimize the influence of the microdefects on the measurement results. This measurement allowed us to estimate the maximal value of the attenuation coefficients at maximal transparency range of few cm-long GaSe and GaSe:Ag crystals as relatively, of 0.1 cm^{-1} and 0.2 cm^{-1}. In Fig. 3 it is seen that absorptivity

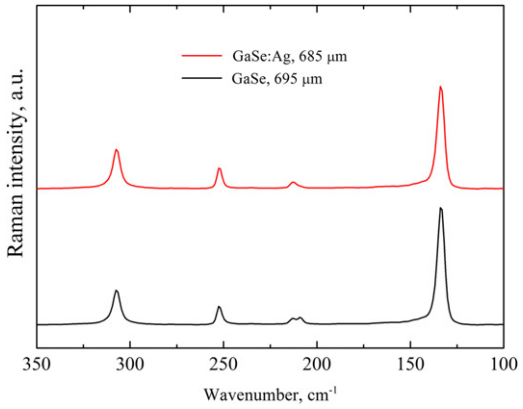

Fig. 2. Raman spectra for GaSe and GaSe:Ag.

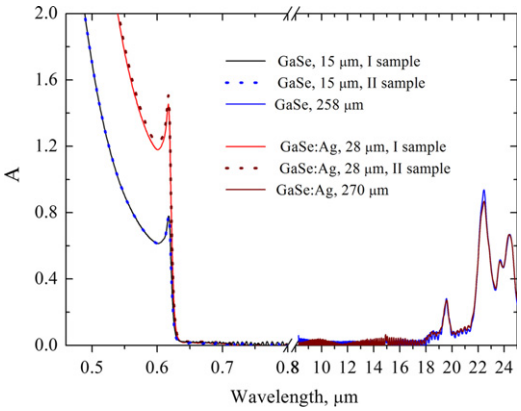

Fig. 3. Optical absorptivity spectra in GaSe and GaSe:Ag crystals.

spectra for GaSe and GaSe:Ag crystals have almost identical spectral features. In our opinion doubled attenuation coefficient in GaSe:Ag is caused sooner by Ag overdoping resulted in microprecipitates observed by scanning electron microscopy (SEM) with LEO 1430 device and small amounts of other defects related to doping. Short-wavelength absorption end of GaSe:Ag crystal is a little bit shifted towards longer wavelength range and something more intensive impurity absorption peak is existing in neighborhood. Small variable density of the precipitates in the crystal bulk leaded to just visible variation in absorptivity of 28 μm samples. THz absorption spectra and dispersion diagrams are displayed in Fig. 4. It is seen that the behavior of absorption spectra and dispersion n_o in GaSe and GaSe:Ag are almost identical, as well as in visible and mid-IR ranges. As to quantitative comparison, the absorption coefficient in GaSe:Ag (Fig. 4a) is two times higher to that in GaSe both in the considered 0.4–2.5 THz range, similar to that in the mid-IR. Dispersion diagram is well in coincidence with the line calculated from dispersion equation recommended in [2], and a little bit ($\delta n = 0.08$) upper to a line estimated from dispersion equations in [43], that did not account phonon absorption mode at 0.59 THz [44,45].

It was found that GaSe:Ag crystal demonstrates no bulk optical damages in contrast to GaSe and even 10–20% higher surface damage threshold. The lack of the bulk damages shows that thermal conductivity in GaSe:Ag is improved to that is GaSe. In turn, it can be proposed that increased surface damage threshold shows improved lattice structure in spite of presence of micro Ag precipitations that do not interact directly with long wavelength CO_2 laser emission.

Due to presence of bulk uniformities of sub-mm dimensions of not identified origin and large work-off effect in GaSe and GaSe:Ag crystals direct quantitative comparison of the SHG efficiencies in 2 mm long GaSe, GaSe:Ag and $ZnGeP_2$ samples was hard to carry out with small cross section pump beam ($<$∅1–2 mm). In the case of pumping by larger (unfocused) ∅6 mm beam with quite uniform energy distribution relative efficiencies in 5.3 mm samples were much more stable during measurements but low efficient due to low intensity. To achieve higher accuracy in comparative study the absence of self-heating effect was controlled by keeping pump power well below the level leading to noticeable changes in phase matching angle and GaSe sample was chosen of the same optical quality as GaSe:Ag. It allowed us to establish that at the same experimental conditions the ratio of non-linear coefficients in chosen GaSe:Ag$GaSe_2$ and GaSe samples is of 0.94 (Fig. 5) in difference to 1.53 reported in [35]. Probably in our case it was governed by Ag over doping leading to formation of something worse quality crystal as it is pointed to above. On the other hand, correspondent loss in figure of merit was even

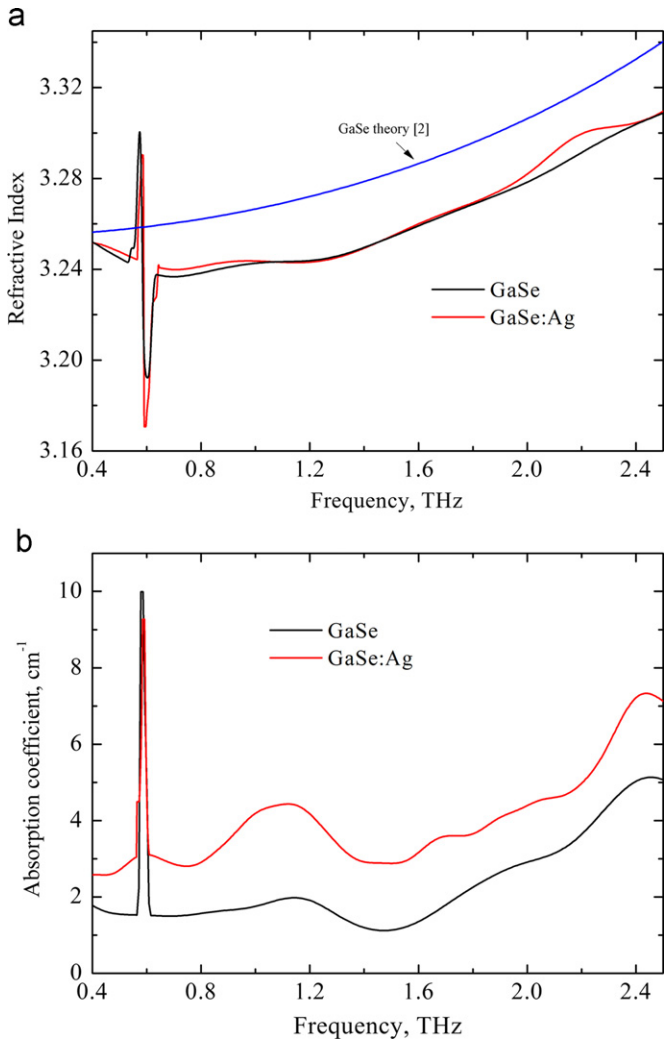

Fig. 4. The THz o-wave dispersion (a) and absorption coefficient spectra (b) in GaSe and GaSe:Ag.

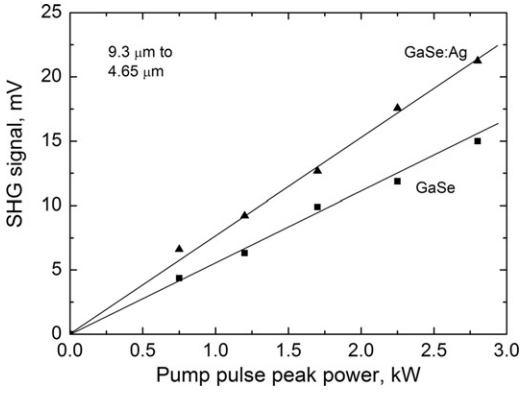

Fig. 5. CO_2 laser SHG signal versus pump pulse peak power. Crystals are identified in the figure inset.

something over compensated by 10–20% higher pump intensity applied permitted by higher damage threshold. So, grown GaSe:Ag crystal is in competition with same quality GaSe crystal and determinately has at least one evident advantage, namely higher hardness.

In this study no attempt was made to reach maximum SHG efficiency neither in $ZnGeP_2$ like in Ref. [4], nor in GaSe:Ag like in other doped GaSe (See Refs. [44,45] but at the maximal pumping intensity $ZnGeP_2$ demonstrated 1.7 times higher CO_2 laser SHG efficiency. GaSe:Ag is characterizing by significantly lower absorption coefficient to that in $ZnGeP_2$ crystals at CO_2 laser wavelengths, 0.2 cm^{-1} versus 0.7 cm^{-1} but $ZnGeP_2$ surfaces were excellent polished due to high hardness, it was highly uniform, as it was determined by method proposed in [41], and possesses higher thermal conductivity. But in our opinion the result achieved in this study can be further improved by optimization of the $AgGaSe_2$ content in the GaSe melt to exclude negative effect of Ag over doping, polishing and cooling that could bring GaSe:Ag crystals in competition with $ZnGeP_2$. In Ref. [35] the sample chosen can be of lower Ag content that is close to optimal doping.

4. Conclusion

Thus it was shown that the crystal grown from the melt GaSe+10 mass% $AgGaSe_2$ is the ε-polytype GaSe crystal doped with silver upto 0.04 mass%. This silver content in GaSe has resulted in 6% decrease in non-linearity that was over compensated in CO_2 laser SHG efficiency by vanishing of the bulk damages and 10–20% improve in the surface damage threshold. This impurity also strengthens the GaSe structure from 8 kg/mm^2 to ≥ 10.7 kg/mm^2 which is promising for cut and polishing at arbitrary direction and applications in out-of-door systems. In difference to $ZnGeP_2$, transparency range of GaSe:Ag allows some body to use visible range reference light beam to control and adjust frequency converter in operation process. It was proposed that the result achieved can be improved by optimal doping, high quality faces polishing and cooling that can bring GaSe:Ag in competition with $ZnGeP_2$ crystal.

Acknowledgment

This work is partially supported by RFBR Project no. 12-08-0042 and Presidium SB RAS IIP No. 46 of 2012.

Reference

[1] G.B. Abdullaev, L.A. Kulevskii, A.M. Prokhorov, A.D. Savel'ev, E.Yu. Salaev, V.V. Smirnov, JETP Letters 16 (1972) 90.
[2] V.G Dmitriev, G.G. Gurzadyan, D.N. Nikogosyan, Handbook of Nonlinear Optical Crystals, Ann Arbor (Michigan Univ), Springer, 1999.
[3] P.G. Schunemann, Recent Advances in Mid-IR Nonlinear Optical Crystals, 〈http://www.onera.fr./jso/opo-2007/pdfs/OPO-IR-ONERA2007-Schunemann.pdf〉.
[4] Y. Jiang, Y.J. Ding, Optics Express 15 (2007) 12699.
[5] A.A. Ionin, I.O. Kinyaevskiy, Yu.M. Klimachev, A.A. Kotkov, A.Yu. Kozlov, Yu.M. Andreev, G.V. Lanskii, A.V. Shaiduko, A.V. Soluyanov, Optics Letters 37 (2012) 2838.
[6] Y. Jiang, Y.J. Ding, Optics Communications 282 (2009) 1452.
[7] W. Shi, X. Mu, Y.J. Ding, N. Fernelius, Applied Physics Letters 80 (2002) 3889.
[8] G.B. Abdullaev, K.R. Allakhverdiev, M.E. Karasev, V.I. Konov, L.A. Kulevskii, N.B. Mustafaev, P.P. Pashinin, A.M. Prokhorov, Yu.M. Starodumov, N.I. Chapliev, Quantum Electronics 19 (1989) 494.
[9] V.A. Gorobets, V.O. Petukhov, S.Ya. Tochitski, V.V. Churakov, Journal of Optical Technology 66 (1999) 53.
[10] K.R. Allakhverdiev, M.Ö. Yetis, S. Özbek, T.K. Baykara, E.Yu. Salaev, Laser Physics 19 (2009) 1092.
[11] W. Shi, Y.J. Ding, N. Fernelius, K.L. Vodopyanov, Optics Letters 27 (2002) 1454.
[12] W. Shi, Y.J. Ding, Applied Physics Letters 84 (2004) 1635.
[13] W. Shi, Y.J. Ding, Optics Letters 30 (2005) 1861.
[14] W. Shi, Y.J. Ding, International Journal of High Speed Electronics and Systems 16 (2006) 589.
[15] Y. Jiang, Y.J. Ding, Applied Physics Letters 91 (2007) 091108/1-3.
[16] W. Shi, Y.J. Ding, N. Fernelius, F.K. Hopkins, Applied Physics Letters 88 (2006) 101101/1-3.
[17] P. Zhao, S.R. Ragam, Y.J. Ding, I.B. Zotova, Optics Letters 35 (2010) 3979.
[18] S.Ya. Tochitsky, C. Sung, S.E. Trubnick, C. Joshi, K.L. Vodopyanov, Journal of the Optical Society of America B 24 (2007) 2509.
[19] W. Shi, Yu.J. Ding, Optics and Photonics News (2002) 57.

[20] Y.-S. Lee, Principle of Terahertz Science and Technology, Springer, New York, 2008.
[21] K.A. Kokh, Yu.M. Andreev, V.A. Svetlichnyi, G.V. Lanskii, A.E. Kokh, Crystal Research and Technology 46 (2011) 327.
[22] D.R. Suhre, N.B. Singh, V. Balakrishna, N.C. Fernelius, F.K. Hopkins, Optics Letters 22 (1997) 775.
[23] Z.-S. Feng, Z.-H. Kang, F.-G. Wu, J.-Yu. Gao, Yu Jiang, H.-Z. Zhang, Yu.M. Andreev, G.V. Lanskii, V.V. Atuchin, T.A. Gavrilova, Optics Express 16 (2008) 9978.
[24] Y.K. Hsu, C.W. Chen, J.Y. Huang, C.L. Pan, J.Y. Zhang, C.S. Chang, Optics Express 14 (2006) 5484.
[25] K.R. Allakhverdiev, R.I. Guliev, E.Yu. Salaev, V.V. Smirnov, Soviet Journal of Quantum Electronics 12 (1982) 947.
[26] L.-M. Zhang, J. Guo, D.-J. Li, J.-J. Xie, Yu.M. Andreev, V.A. Gorobets, V.V. Zuev, K.A. Kokh, G.V. Lanskii, V.O. Petukhov, V.A. Svetlichnyi, A.V. Shaiduko, Journal of Applied Spectroscopy 77 (2011) 850.
[27] Z. Rak, S.D. Mahanti, K.C. Mandal, N.C. Fernelius, Physical Review B 82 (2010) 155203/1-10.
[28] Y. Qu, Z.-H. Kang, T.-J. Wang, Yu.M. Andreev, G.V. Lanskii, A.N. Morozov, S.Yu. Sarkisov, Atmospheric and Oceanic Optics 21 (2008) 146.
[29] Yu.M. Andreev, Modified Non-Linear Crystals GaSe: Physical Properties and Application, In: Proceedings of the X International Conference on Atomic and Molecular Pulsed Lasers, September 12–16, 2011, Tomsk, Russia. Conference Abstracts. IOA SB RAS (2011), pp. 137.
[30] S. Das, C. Ghosh, O.G. Voevodina, Yu.M. Andreev, S.Yu. Sarkisov, Applied Physics B 82 (2006) 43.
[31] G.V. Mayer, T.N. Kopylova, Yu.M. Andreev, V.A. Svetlichnyi, E.N. Tel'minov, Russian Physics Journal 52 (2009) 640.
[32] L.-L. Chu, I.-F. Zhang, Zh.H. Kang, Y. Jiang, J.Y. Gao, Yu.M. Andreev, E.M. Vinnik, V.V. Zuev, K.A. Kokh, G.V. Lansky, A.N. Morozov, A.V. Shaiduko, Russian Physics Journal 53 (2011) 1235.
[33] Z.-S. Feng, J. Guo, Z.-H. Kang, Y. Jiang, J.-Y. Gao, J.-J. Xie, L.-M. Zhang, V. Atuchin, Y. Andreev, G. Lanskii, A. Shaiduko, Applied Physics, doi:10.1007/s00340-012-5067-9, in press.
[34] Y.-F. Zhang, R. Wang, Z.-H. Kang, L.-L. Qu, Y. Jiang, J.-Y. Gao, Yu.M. Andreev, G.V. Lanskii, K.A. Kokh, A.N. Morozov, A.V. Shaiduko, V.V. Zuev, Optics Communications 284 (2011) 1677.
[35] N.B. Singh, D.R. Suhre, W. Rosch, R. Meyer, M. Marable, N.C. Fernelius, F.K. Hopkins, D.E. Zelmon, R. Narayanan, Journal of Crystal Growth 198 (1999) 588.
[36] K.A. Kokh, Yu.M. Andreev, V.A. Svetlichnyi, G.V. Lanskii, A.E. Kokh, Crystal Research and Technology 46 (2011) 327.
[37] D.R. Suhre, N.B. Singh, V. Balakrishna, N.C. Fernelius, F.K. Hopkins, Optics Letters 22 (1997) 775.
[38] K.A. Kokh, B.G. Nenashev, A.E. Kokh, G.Yu. Shvedenkov, Journal of Crystal Growth 275 (2005) e2129.
[39] M.M. Nazarov, S.A. Makarova, A.P. Shkurinov, O.G. Okhotnikov, Applied Physics Letters 92 (2008) 021114/1-3.
[40] Yu.M. Andreev, K.A. Kokh, G.V. Lanskii, A.N. Morozov, Journal of Crystal Growth 318 (2011) 1164.
[41] M. Hayek, O. Brafman, R.M.A. Lieth, Physical Review B 8 (1973) 2772.
[42] H. Yoshida, S. Nakashima, A. Mitsuishi, Physica Status Solidi B 59 (1973) 655.
[43] K.R. Allakhverdiev, T. Baykara, A. Kulibekov Gulubayov, A.A. Kaya, J. Goldstein, N. Fernelius, S. Hanna, Z. Salaeva, Journal of Applied Physics 98 (2005) 093515/1-6.
[44] W.-C. Chu, S.A. Ku, H.J. Wang, C.W. Luo, Yu.M. Andreev, G. Lanskii, T. Kobayashi, Optics Letters 37 (2012) 945.
[45] S.-A. Ku, W.-C. Chu, C.-W. Luo, Y. Andreev, G. Lanskii, A. Shaiduko, T. Izaak, V. Svetlichnyi, Optics Express 20 (2012) 5029.